

- (6) The molecular geometry was generated using standard bond-length and bond-angle values from J. A. Pople and D. L. Beveridge, "Approximate Molecular Orbital Theory", McGraw-Hill, New York, 1970, pp 111–112.
- (7) A. C. Shapski and J. L. Stevenson, *J. Chem. Soc., Perkin Trans. 2*, 1197 (1973). Amino and phenyl hydrogen bond lengths and angles were taken from K. Trueblood, E. Goldish, and J. Donohue, *Acta Crystallogr.*, **14**, 1009 (1961).
- (8) The oscillator strength of the transition ${}^1\Gamma_1 \leftarrow {}^1\Gamma_1$ is referred to here and elsewhere as $f({}^1\Gamma_1)$.
- (9) T. P. Carsey, Ph.D. Dissertation, Louisiana State University, Baton Rouge, 1977.
- (10) V. G. Plotnikov and V. M. Komarov, *Spectrosc. Lett.*, **9**, 265 (1976).
- (11) M. F. A. El-Sayed, *J. Chem. Phys.*, **38**, 2834 (1963).
- (12) O. S. Khalil and S. P. McGlynn, *J. Lumin.*, **11**, 185 (1975–1976).

Crystal and Molecular Structure of $[n\text{-Bu}_4\text{N}^+][\text{S}_3\text{N}_3^-]$ and the Vibrational Assignments and Electronic Structure of the Planar Six-Membered Ring of the Trisulfur Trinitride Anion

J. Bojes, T. Chivers,* W. G. Laidlaw, and M. Trsic

Contribution from the Department of Chemistry, University of Calgary, Calgary T2N 1N4, Alberta, Canada. Received October 10, 1978

Abstract: The crystal and molecular structure of $[n\text{-Bu}_4\text{N}^+][\text{S}_3\text{N}_3^-]$ has been determined by X-ray crystallography. The compound crystallizes in the space group $P2_1/n$, $a = 9.074$ (5) Å, $b = 15.901$ (12) Å, $c = 15.389$ (6) Å, $\beta = 98.98$ (4)°, $V = 2193$ Å³, and $Z = 4$. The refined structure ($R = 0.097$) shows that the S_3N_3^- ion is a six-membered, essentially planar ring with S–N distances in the range 1.580 (13) to 1.626 (12) Å. The bond angles within the ring at nitrogen are 122.6 (8)–124.2 (9)° and at sulfur they are 116.5–117.0 (7)°. The infrared and Raman spectra of alkali metal and tetraalkylammonium salts of S_3N_3^- are discussed and assigned on the basis of D_{3h} symmetry for the anion. Ab initio Hartree–Fock–Slater SCF calculations have been carried out for S_3N_3^- and show (a) that a planar configuration is of lower energy than other ring conformations and (b) that the ground-state electronic structure is a 10π system with a net of one π bond distributed over the six S–N bonds of the ring. Assuming the corresponding cation, S_3N_3^+ , to have a planar (D_{3h}) geometry, similar calculations predict this species to be a diradical. Calculations of the energy and oscillator strengths for the lowest allowed electronic transitions of S_3N_3^- lead to the assignment of the 360-nm peak in the electronic spectrum to a $\pi^* \rightarrow \pi^*$ transition (calculated wavelength 399 nm).

Introduction

Recently the synthesis and characterization of cesium and tetraalkylammonium salts of the novel sulfur–nitrogen anion, S_3N_3^- , from the reaction of the appropriate azide with S_4N_4 in ethanol were reported.¹ The vibrational spectra of these salts suggested a six-membered ring structure for S_3N_3^- , in contrast to the five-membered ring structure established for the iso-electronic cation, $\text{S}_3\text{N}_2\text{Cl}^+$,² and also found in a number of S_3N_3 derivatives, e.g., $\text{S}_3\text{N}_3\text{COCF}_3$.³ In the particular case of the cesium salt, we concluded from the vibrational spectra that the ring in S_3N_3^- was puckered (C_{3v}).¹ Six years ago, in a discussion of his proposals for "electron-rich aromatic" S–N species, Banister wrote "it is not known whether an anionic charge (e.g. as in S_3N_3^-) has a serious destabilizing effect on sulphur d_π bonding, as no planar anions have been prepared."^{4,5} Since a knowledge of the structure is an essential prerequisite to a discussion of the bonding in S_3N_3^- , an X-ray structural determination of $n\text{-Bu}_4\text{N}^+\text{S}_3\text{N}_3^-$ was undertaken and the details are reported here together with the vibrational assignments for the S_3N_3^- . In addition, we have carried out ab initio Hartree–Fock–Slater (HFS) SCF calculations of the ground-state electronic structure of S_3N_3^- (and of the related cation S_3N_3^+) in order to (a) determine the relative energies of various ring geometries, (b) ascertain that the planar anion is a Hückel-type (10π) system, (c) assign the 360-nm band observed in the UV–visible spectrum of S_3N_3^- to the appropriate electronic transition.

Experimental Section

Crystal Preparation. $[\text{Bu}_4\text{N}^+][\text{S}_3\text{N}_3^-]$ was prepared from tetra-*n*-butylammonium azide and S_4N_4 in ethanol, as previously de-

scribed.^{1b} Yellow prisms suitable for X-ray diffraction studies were obtained by the rapid evaporation (3–4 h) of a solution in absolute ethanol at 0 °C in a stream of nitrogen. The dimensions of the crystal used in this study were 0.3 × 0.3 × 0.35 mm. All manipulations were carried out under an atmosphere of dry nitrogen in view of the sensitivity of S_3N_3^- salts to air oxidation, particularly in solution. In one attempted recrystallization of $[\text{Me}_4\text{N}^+][\text{S}_3\text{N}_3^-]$, during which an ethanol solution was allowed to stand for 24 h, white crystals of tetramethylammonium tetrathionate were obtained and identified by infrared bands at 1025 s, 620 s, 535 s, 525 s, 485 w, 460 w, and 370 w cm^{-1} and by elemental analysis. Anal. Calcd for $\text{C}_8\text{H}_{24}\text{N}_2\text{S}_4\text{O}_6$: C, 25.79; H, 6.51; N, 7.52; S, 34.42; O, 25.76. Found: C, 25.42; H, 6.71; N, 7.53; S, 34.41; O, 25.93 (by difference).

Crystal Data. $[\text{Bu}_4\text{N}^+][\text{S}_3\text{N}_3^-]$, mol wt 380.68, monoclinic. For calculation of cell constants, 25 reflections were computer centered and the setting angles were least-squares refined. The following systematic absences were observed: $h0l$, $h + l \neq 2n$; $0k0$, $k \neq 2n$. The cell constants are $a = 9.075$ (5) Å, $b = 15.901$ (12) Å, $c = 15.389$ (6) Å, $V = 2193$ Å³, $Z = 4$, $d_c = 1.152$ g cm^{-3} , space group $P2_1/n$.

X-ray Measurements. Intensity data were collected at 23 ± 1 °C using graphite monochromated Mo $K\alpha$ radiation ($\lambda = 0.71069$ Å) and a θ - 2θ scan rate varying from 4 to 24°/min, depending on the intensity of the reflection. Stationary background counts with a time equal to half the scan time for each reflection were made at each end of the scan range. The scan range varied from -0.5° at low 2θ to $+0.5^\circ$ for the higher angle data. Of the 3951 reflections collected in the range $0^\circ < 2\theta$ (Mo $K\alpha$) $< 50^\circ$, 3374 unique reflections with $I > 3\sigma(I)$ were retained as observed and corrected for Lorentz and polarization effects. Three representative reflections were measured periodically to check crystal and electronic stability, but no significant change in intensity was observed. The linear absorption coefficient of this compound is 3.34 cm^{-1} for Mo $K\alpha$ radiation and no absorption correction was necessary.

Solution and Refinement of the Structure. The structure was solved by direct methods. Using 312 reflections ($E_{\text{min}} = 1.40$) and 2000 phase relationships, a total of 16 phase sets were produced. An E map pre-

Table I

A. Final Positional Parameters for S ₃ N ₃ ⁻ in [Bu ₄ N ⁺][S ₃ N ₃ ⁻] ^a			
atom	x	y	z
S(1)	0.3054(7)	0.1660(4)	0.1377(4)
S(2)	0.4535(7)	0.3204(4)	0.1779(4)
S(3)	0.6188(7)	0.1735(5)	0.1617(5)
N(1)	0.304(2)	0.266(1)	0.1545(11)
N(2)	0.606(2)	0.272(1)	0.1815(12)
N(3)	0.468(2)	0.123(1)	0.1369(11)

B. Anisotropic Thermal Parameters (Å ²) for S ₃ N ₃ ⁻ in [Bu ₄ N ⁺][S ₃ N ₃ ⁻] ^{a,b}						
atom	B ₁₁	B ₂₂	B ₃₃	B ₁₂	B ₁₃	B ₂₃
S(1)	0.023(1)	0.0079(4)	0.0084(4)	-0.009(1)	0.006(1)	-0.0003(8)
S(2)	0.026(1)	0.0054(3)	0.0102(5)	0.004(1)	0.002(1)	-0.0037(8)
S(3)	0.023(1)	0.0080(4)	0.0104(4)	0.013(1)	-0.004(1)	-0.0031(9)
N(1)	6.9(5)					
N(2)	7.9(5)					
N(3)	6.7(5)					

^a Positional and thermal parameters of the Bu₄N⁺ cations can be found in the supplementary material. ^b The form of the anisotropic thermal parameter is $\exp[-B_{11}h^2 + B_{22}k^2 + B_{33}l^2 + B_{12}hk + B_{13}hl + B_{23}kl]$.

pared from the phase set showing the best probability statistics (absolute figure of merit = 0.85, residual = 37.7) a total of 18 atoms were located. These atoms were included in least-squares refinement, resulting in agreement factors of $R_1 = 0.31$ and $R_2 = 0.40$. The remaining nonhydrogen atoms were located in succeeding difference Fourier syntheses.

In full-matrix least-squares refinement the function minimized was $\sum w(|F_o| - |F_c|)^2$ where the weight w is defined as $4F_o^2/\sigma^2(F_o^2)$. Scattering factors were taken from Cromer and Waber.⁶ Anomalous dispersion effects were included in F_c ; the values of $\Delta f'$ and $\Delta f''$ were those of Cromer and Liberman.⁷ Only the 714 reflections having $F_o^2 > 3\sigma(F_o^2)$ were used in the refinement. The following values pertain to the final cycle of least-squares refinement.

$$R_1 = \sum |F_o| - |F_c| / \sum |F_o| = 0.097$$

$$R_2 = [\sum w(|F_o| - |F_c|)^2 / \sum wF_o^2]^{1/2} = 0.115$$

The final difference Fourier map showed no significant residual electron density, except for hydrogen atoms on the *n*-butyl groups. The highest peak was $1.2 \text{ e } \text{Å}^{-3}$ and was 0.5 Å from S(2). No unusual trends were observed in an analysis of $\sum w(F_o - F_c)^2$ vs. F_o , $\lambda^{-1} \sin \theta$, or various classes of indices. A list of observed and calculated structure factor tables is available.⁸

Infrared and Raman Spectra. Infrared spectra (4000–250 cm^{-1}) were recorded as Nujol mulls (CsI optics) on a Perkin-Elmer 467 spectrophotometer, and far-infrared spectra (665–40 cm^{-1} , polyethylene windows) were measured using a Digilab FTS 16 instrument. Raman spectra were obtained on samples sealed in capillaries under nitrogen using argon (5145 Å) and He/Ne (6328 Å) lasers and a Jarrell-Ash spectrophotometer and were calibrated against carbon tetrachloride. The preparative routes to the various S₃N₃⁻ salts are described in ref 1 and 19.

Ultraviolet-Visible Spectra. A solution of Me₄N⁺S₃N₃⁻ in dry absolute ethanol ($2.19 \times 10^{-4} \text{ M}$) was prepared in a Vacuum Atmospheres drybox. An aliquot of this solution was transferred to a 1.0-cm quartz cell equipped with nitrogen purge (Airless ware) and the UV-visible spectrum was recorded on a Cary 15 spectrophotometer.

Theoretical Method

The closed-shell HFS one-electron equations⁹ in which the exchange term is substituted by the "Slater exchange" term

$$V_{\text{HFS}}(1) = -3\alpha[(3/4\pi)\rho(1)]^{1/3} \quad (1)$$

where ρ is the one-electron density, were solved in the manner described elsewhere^{10,11} with $\alpha = 0.7$. This ab initio procedure has been widely tested for the calculation of molecular properties¹² and the results suggest a high degree of reliability. The total statistical energy was calculated with a procedure recently

Table II. Bond Lengths (Å) and Angles (deg) of (*n*-C₄H₉)₄N⁺ in [*n*-Bu₄N⁺][S₃N₃⁻]

N(4)-C(1)	1.562(13)	C(6)-C(7)	1.626(15)
N(4)-C(5)	1.542(12)	C(7)-C(8)	1.56(2)
N(4)-C(9)	1.567(13)	C(9)-C(10)	1.518(15)
N(4)-C(13)	1.558(13)	C(10)-C(11)	1.597(15)
C(1)-C(2)	1.55(2)	C(11)-C(12)	1.57(2)
C(2)-C(3)	1.70(2)	C(13)-C(14)	1.56(2)
C(3)-C(4)	1.44(2)	C(14)-C(15)	1.67(2)
C(5)-C(6)	1.562(14)	C(15)-C(16)	1.50(2)
C(1)-N(4)-C(5)	112.6(8)	N(4)-C(5)-C(6)	111.6(9)
C(1)-N(4)-C(9)	101.4(9)	C(5)-C(6)-C(7)	102(1)
C(1)-N(4)-C(13)	113.5(9)	C(6)-C(7)-C(8)	106(1)
C(5)-N(4)-C(9)	112.6(9)	N(4)-C(9)-C(10)	111(1)
C(5)-N(4)-C(13)	103.6(8)	C(9)-C(10)-C(11)	105(1)
C(9)-N(4)-C(13)	113.5(8)	C(10)-C(11)-C(12)	110(1)
N(4)-C(1)-C(2)	108(1)	N(4)-C(13)-C(14)	109(1)
C(1)-C(2)-C(3)	106(1)	C(13)-C(14)-C(15)	104(1)
C(2)-C(3)-C(4)	111(1)	C(14)-C(15)-C(16)	110(1)

^a Numbering scheme: The N atom of the (*n*-C₄H₉)₄N⁺ cation is N(4). The carbon atoms of each *n*-C₄H₉ group are labeled C(1), C(2), C(3), C(4), etc., with the lowest number carbon atom of each set of four being attached to nitrogen.

described¹³ and used as a probe for molecular conformation.

A double ζ Slater type set of orbitals¹⁴ (STO) was employed, augmented, in the case of the sulfur atom, with a 3d orbital with exponent 1.68¹⁵ while the 1s² core of nitrogen and the 1s² 2s² 2p⁶ core of sulfur were kept "frozen"¹⁰ during the variational procedure.

Results and Discussion

Crystal Structure of [*n*-Bu₄N⁺][S₃N₃⁻] and the Conformation of the S₃N₃⁻ Ring. The positional and thermal parameters for the anion in *n*-Bu₄N⁺S₃N₃⁻ are given in Table I. Bond lengths and bond angles together with the numbering scheme for the *n*-Bu₄N⁺ cation are summarized in Table II. Bond lengths and bond angles for the S₃N₃⁻ anion are depicted in Figure 1. The structure determination has confirmed the proposed six-membered ring of S₃N₃⁻ with S-N bond lengths in the range 1.584–1.626 Å (only just outside the 3σ criterion of significance). The S₃N₃⁻ ring is essentially planar, the maximum deviation from the least-squares plane through all six atoms being 0.057 Å for N₃ (Table III). Inspection of

Table III. Weighted Least-Squares Planes for S_3N_3^- ^a

atom	dev, Å	atom	dev, Å
S(1)	-0.010(7)	N(1)	0.028(16)
S(2)	0.002(7)	N(2)	-0.027(18)
S(3)	-0.003(7)	N(3)	0.057(16)

^a Equation of the plane is $0.1222x + 0.1851y - 0.9751z + 1.2434 = 0$.

nonbonded intermolecular contacts up to 4 Å (see supplementary material) reveals no significant interactions between atoms of the anion and atoms of the cation. As a result of the planar configuration of the S_3N_3^- ring the bond angles at nitrogen are ca. 123° and at sulfur they are ca. 117°, indicating significant strain in the ring.¹⁶ Presumably this is compensated, in part, by the stabilization energy resulting from a planar ring. The HFS procedure outlined in the preceding section can be made to yield¹³ the molecular (including nuclear repulsions) energy. This energy was calculated¹⁷ for a number of conformations of the S_3N_3^- ring and the planar form (D_{3h}) was always lower. For example, the chair form with S-N bond distances of 1.62 Å and angles at N of 123° and at S of 109° was 13 kcal mol⁻¹ higher than the planar conformation with equal S-N bond distances and bond angles of 120° at S and N. Puckered forms (C_{3v}) were 8–10 kcal mol⁻¹ and a boat configuration was ca. 30 kcal mol⁻¹ higher in energy than the planar form. Though not an exhaustive search, these results, together with the X-ray analysis, do indicate that the counterion, $n\text{-Bu}_4\text{N}^+$, does not prejudice the structure of the S_3N_3^- ring. However, the vibrational spectral data described in the next section suggest that this is not always the case, e.g., with Cs^+ as counterion. It is noteworthy that recent CNDO/2 MO calculations for S_4N_2 (isoelectronic with S_3N_3^-) also show that the planar ring structure is favored over any nonplanar geometry.¹⁸

Several attempts to obtain suitable crystals of an S_3N_3^- salt for an X-ray structure determination were made before success was achieved. We were unable to obtain satisfactory crystals of $\text{Cs}^+\text{S}_3\text{N}_3^-$ by recrystallization from absolute methanol. In the case of $[\text{Me}_4\text{N}^+][\text{S}_3\text{N}_3^-]$ preliminary X-ray data were collected which indicated that the structure was highly disordered. During the recrystallization of $[\text{Me}_4\text{N}^+][\text{S}_3\text{N}_3^-]$ it was found that solutions which were stored in ethanol under nitrogen for 24 h produced tetramethylammonium tetrathionate, $[\text{Me}_4\text{N}^+]_2[\text{S}_4\text{O}_6^{2-}]$, and S_4N_4 .

Vibrational Assignments for the S_3N_3^- Anion. In a previous paper^{1b} we reported the infrared and Raman spectra of $\text{Cs}^+\text{S}_3\text{N}_3^-$ and concluded that the S_3N_3^- anion in the cesium salt was a six-membered ring with a puckered conformation (C_{3v}). Since a planar configuration has been found for S_3N_3^- in the $n\text{-Bu}_4\text{N}^+$ salt by X-ray crystallography, we have now investigated the infrared and Raman spectra of all the available S_3N_3^- salts^{1,19} in detail to determine whether the vibrational spectra are consistent with D_{3h} symmetry for the anion in R_4N^+ salts and to probe the possibility of anion-cation interactions leading to a lowering of the symmetry of the anion, e.g., in alkali metal salts. The results are summarized in Table IV. From these data it is clear that the infrared spectra of S_3N_3^- salts are characterized by three strong bands at ca. 925, 640, and 380 cm⁻¹. A fourth band at ca. 170–190 cm⁻¹ was observed in the far-infrared spectra of the potassium and cesium salts. A further two very weak bands at ca. 590 and 690 cm⁻¹^{1b} appear in all samples of $\text{Cs}^+\text{S}_3\text{N}_3^-$ that we have prepared.⁴² These bands were absent, however, in the infrared spectra of the sodium and potassium salts.

In order to avoid decomposition, sometimes with explosion, in the measurement of Raman spectra it was necessary to focus the laser beam on only a small portion of the sample in the

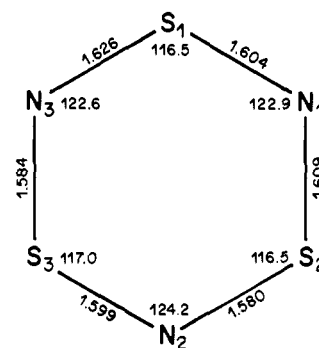
Structure of the S_3N_3^- anion

Figure 1. Bond lengths (in Å with esd's of 0.012 Å) and bond angles (in degrees with esd's of 0.7° at S and 0.8° at N) of the S_3N_3^- anion in $[n\text{-Bu}_4\text{N}^+][\text{S}_3\text{N}_3^-]$.

capillary tube. All of the R_4N^+ salts decomposed (black coloration) in the 5145-Å (green) laser line, but satisfactory spectra were obtained using the 6471-Å (red) exciting wavelength. A Raman spectrum for $[\text{Me}_4\text{N}^+][\text{S}_3\text{N}_3^-]$ in methanol was obtained, although decomposition was evident after 1 h as indicated by the growth of bands at 711 or 1030 cm⁻¹ at the expense of bands attributable to S_3N_3^- . It was not possible to obtain solution Raman spectra for the alkali metal salts, owing to poor solubility. The data in Table IV show that the Raman spectra of S_3N_3^- salts are characterized by five bands at ca. 925 s, 700 w, 645 w, 590 vs, and 375 m cm⁻¹, three of which show coincidences in the infrared spectrum. It is possible that a sixth Raman band below 200 cm⁻¹ is obscured by the lattice mode at 140 cm⁻¹. Thus, the vibrational spectra for $\text{K}^+\text{S}_3\text{N}_3^-$ (and the R_4N^+ salts) are consistent with a structure of D_{3h} symmetry for the anion, since group theory predicts four infrared-active modes, six Raman-active modes, and three coincidences for D_{3h} symmetry.^{1b}

Vibrational assignments have been made for a number of species structurally similar to S_3N_3^- . For example, a planar ring structure (D_{3h}) was assigned to Si_3O_3 on the basis of the infrared spectrum supported by force-field calculations.²⁰ More recently P_3N_3 , formed by the aggregation of matrix-isolated PN monomer units, was detected and shown to have D_{3h} symmetry on the basis of infrared spectra of isotopically enriched (¹⁵N) samples.²¹ For Si_3O_3 and P_3N_3 , vibrational assignments are based on infrared spectra only. More complete vibrational analyses have been reported, however, for mixed trimeric phosphonitrilic halides of the type $\text{N}_3\text{P}_3\text{X}_n\text{Y}_{n-6}$ (X = Cl; Y = Br²² or F;²³ n = 0–6) in which the N_3P_3 ring is assumed to be planar.

The assignments of the vibrational modes for S_3N_3^- , according to their notation under D_{3h} symmetry,²² are given in Table IV. According to Coxon and Sowerby,²² the expected vibrational modes and activities for a planar, six-membered ring are as follows:

ring stretching $A_1'(R) + A_2'(inactive) + 2E'(IR, R)$

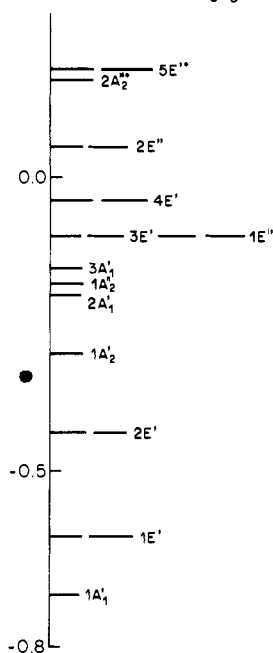
ring deformation $A_1'(R) + A_2''(IR) + E'(IR, R) + E''(R)$

There are only two symmetric A_1' vibrations. These are the symmetric stretching breathing, ν_1 , and the in-plane bending trigonal deformation, ν_2 , vibration. These bands are Raman allowed and infrared forbidden and they occur as a weak band at ca. 700 cm⁻¹ (ν_1) and as a very strong, polarized band at ca. 590 cm⁻¹ (ν_2) in the Raman spectra of S_3N_3^- salts. It is significant that both of these vibrations are apparently observed as weak bands at ca. 695 and 590 cm⁻¹, respectively,^{1b} in the infrared spectrum of the cesium salt indicating a lowering of

Table IV. Raman and Infrared Spectra (cm^{-1}) of Salts of the S_3N_3^- Ion and Their Assignments

NaS_3N_3^a IR (mull)	KS_3N_3		CsS_3N_3		$\text{Me}_4\text{NS}_3\text{N}_3^b$			assignments ^c
	IR (mull)	Raman (solid)	IR (mull)	Raman (solid)	IR (mull)	Raman (solid)	Raman (soln)	
			76 s ^d					
	125 s ^d		89 sh ^d		130 m			
	187 s		168 s					$\text{A}_2''(\nu_5)$, op
380 s	385 m	371 m	370 s	371 m	380 m	376 w	384 w, dp	$\text{E}'(\nu_{13})$, ip
		594 vs	590 vw	587 vs		587 vs	589 vs. p	$\text{A}_1'(\nu_2)$
640 vs	640 vs	643 vw	645 vs	644 w	640 vs	644 w	644 vw ^e	$\text{E}'(\nu_{12})$
		703 w	690 vw	697 w				$\text{A}_1'(\nu_1)$
							711 s ^f	
920 s	925 s	926 vs	925 s	928 vs	920 s	922 s	922 m, dp	$\text{E}'(\nu_{11})$, ip
							1030 m ^f	

^a Raman and far-IR spectra were not obtained for the Na^+ salt. ^b Other R_4N^+ ($\text{R} = \text{Et}, n\text{-Pr}, n\text{-Bu}$) showed bands at ca. 925 m, 640 vs, and 385 cm^{-1} in addition to bands due to the cation. ^c Notation for D_{3h} ; the $\text{E}''(\nu_{18})$ mode is probably obscured by a lattice mode at 140 cm^{-1} . ^d Lattice mode. ^e This Raman mode was too weak for its degree of polarization to be measured. ^f These bands result from decomposition of S_3N_3^- in the laser beam.

ORBITAL ENERGIES OF S_3N_3^- (a.u.)Figure 2. Orbital energy level diagram for planar (D_{3h}) S_3N_3^- .

the symmetry of the anion in this salt. The $\text{A}_2''(\nu_9)$ trigonal S-N stretching mode is completely inactive in molecules with D_{3h} symmetry.²²

The E' modes (ν_{11} , ν_{12} , ν_{13}) are in-plane ring vibrations which are coincident in the Raman and infrared spectra. The first two are asymmetric stretching ring vibrations observed at ca. 925 and 640 cm^{-1} . Resolution of the degeneracy of these vibrations is not observed for either of these bands in any salts, except that the usually broad infrared band at ca. 645 cm^{-1} in $\text{Cs}^+\text{S}_3\text{N}_3^-$ was sometimes resolved into a doublet. The third E' vibration, ν_{13} , is the in-plane bending vibration and occurs at ca. 380 cm^{-1} . Both the 925- and 380- cm^{-1} bands are depolarized in the solution Raman spectrum of $[\text{Me}_4\text{N}^+][\text{S}_3\text{N}_3^-]$, but the 640- cm^{-1} peak was too weak to determine the degree of polarization.

The $\text{A}_2''(\nu_5)$ and $\text{E}''(\nu_{18})$ modes are out-of-plane deformation vibrations and are expected to occur at lower frequencies than the in-plane modes. Hence, ν_5 , which should be infrared active only, has been assigned to the band at 187 cm^{-1} in the far-infrared spectrum of $\text{K}^+\text{S}_3\text{N}_3^-$. The ν_{18} vibration, which should only be Raman active, was not observed,

possibly because it was obscured by the lattice mode at ca. 140 cm^{-1} in the Raman spectrum. Finally, no combination or overtone bands were observed in the vibrational spectra of S_3N_3^- salts.

In summary, the vibrational spectra of sodium, potassium, and tetraalkylammonium salts of S_3N_3^- are consistent with a structure of D_{3h} symmetry for the anion. Vibrational assignments have been made assuming this symmetry. In the particular case of the cesium salt, the vibrational spectra indicate that the symmetry of the S_3N_3^- anion is lower than D_{3h} .

Electronic Structure and Bonding in S_3N_3^- . Although examples of planar, monocyclic S-N cations, e.g., S_4N_3^+ and S_5N_5^+ , are well-known, S_3N_3^- is the first example of a planar, cyclic S-N anion. According to the proposals of Banister,⁵ this species should be a 10π -electron Hückel-type system.

In order to obtain the electronic description of S_3N_3^- , we applied the ab initio HFS-SCF procedure to a planar S_3N_3^- ring with S-N bond distances of 1.60 Å and bond angles of 120° at S and N. There are 34 electrons in S_3N_3^- which are external to the frozen core. An orbital energy level diagram for planar S_3N_3^- is shown in Figure 2 and orbital overlap populations²⁴ are provided in Table V.

The lowest lying orbital $1\text{A}_1'$ utilizes s-type STOs from all six centers and generates, as Table V shows, positive overlap (0.031) between nearest neighbors—it is a σ -type bonding orbital. The eight electrons in $1\text{E}'$ and $2\text{E}'$ utilize s and p combinations to generate bonding density in the plane of the molecule. The $1\text{A}'$ orbital utilizes in-plane p orbitals (p_x and p_y) to generate yet another σ -bonding contribution between adjacent S and N. The $2\text{A}_1'$ orbital is a clearly defined sulfur lone-pair orbital (cf. the virtually zero entries in Table V for overlap between N centers and the large (0.25) entry for the sulfur centers). The last of the occupied A_1' orbitals, $3\text{A}_1'$, is strongly antibonding (-0.060) for adjacent S and N. Finally, the four electrons in $3\text{E}'$ contribute to σ bonding while the four electrons in $4\text{E}'$ make an antibonding contribution. The picture which emerges is that of four strong σ bonds ($1\text{A}_1'$, $1\text{E}_1'$, $1\text{E}_2'$, and $1\text{A}_2'$) with the weaker σ -bonding contribution of $2\text{E}_1'$, $2\text{E}_2'$, $3\text{E}_1'$, and $3\text{E}_2'$ being largely offset by the antibonding of $3\text{A}_1'$, $4\text{E}_1'$, and $4\text{E}_2'$. It is also clear that, in addition to the sulfur lone-pair orbital $2\text{A}_1'$, other orbitals, such as $4\text{E}'$, which is weakly antibonding, or $3\text{E}'$, which is weakly bonding, must be recognized as having lone-pair characteristics. For example, for $4\text{E}'$, the large entry of 0.268 under N signals lone-pair character in addition to the antibonding character. Thus, there are lone-pair-like electrons but they are carried in distributions with bonding or antibonding character.

The first π orbital of S_3N_3^- , $1\text{A}_2''$, is composed of positive

Table V. Overlap Population

MO (<i>i</i>) designation		orbital overlap populations $P_{rs}(i)$				orbital overlap populations $P_{rr}(i)$	
symmetry	dominant features	SN _a ^a	SS _b ^b	NN _b ^b	SN _b ^b	N	S
1A ₁ '	σ	0.031	0.005	0.007	0.003	0.110	0.071
2A ₁ '	lpS	0.005		0.003	0.003	0.047	0.251
3A ₁ '	σ*	-0.060	0.023	0.006	-0.006	0.321	0.206
1A ₂ '	σ	0.031	-0.010	-0.003	0.002	0.123	0.112
1E ₁ '	σ	0.031		-0.003	-0.003	0.140	0.079
1E ₂ '	σ	0.031		-0.003	-0.003	0.140	0.079
2E ₁ '	σ, lpS	0.019	-0.015	-0.003	0.003	0.103	0.185
2E ₂ '	σ, lpS	0.019	-0.015	-0.003	0.003	0.103	0.185
3E ₁ '	σ, lpS	0.013	-0.010	-0.001	-0.007	0.100	0.222
3E ₂ '	σ, lpS	0.013	-0.010	-0.001	-0.007	0.100	0.222
4E ₁ '	σ*, lpN	-0.022	0.005	0.001	-0.001	0.268	0.143
4E ₂ '	σ*, lpN	-0.022	0.005	0.001	-0.001	0.268	0.143
1A ₂ ''	π	0.024	0.010	0.001	0.002	0.087	0.123
1E ₁ ''	π	0.020	-0.003	-0.001	-0.002	0.124	0.144
1E ₂ ''	π	0.020	-0.003	-0.001	-0.002	0.124	0.144
2E ₁ ''	π*, lpS	-0.012	-0.012	-0.001	0.003	0.150	0.251
2E ₂ ''	π*, lpS	-0.012	-0.012	-0.001	0.003	0.150	0.251
net population		0.52 ^c	-0.17 ^c	-0.01 ^c	-0.05 ^c	4.92 ^d	5.61 ^d

^a Refers to adjacent atoms. ^b Refers to cross-ring interactions. ^c Indicates the overlap populations and is given by four times the column sum where the 4 arises due to doubly occupied orbitals giving a factor of 2 and the quadratic form of the population giving rise to another factor of 2 for the cross terms. ^d Indicates the partial atomic population () and since all orbitals are doubly occupied is two times the column sum.

p_z contributions from all centers and provides a strong (0.024) π -bonding contribution. The degenerate 1E'' pair of π orbitals makes a bonding contribution of 0.021 while the negative contribution of -0.012 characterizes the 2E' orbitals as antibonding, i.e., π^* orbitals. The picture which emerges here is clearly that of a 10 π electron system of six centers. The occupancy of the antibonding orbitals reduces the π bonding to a net of a little over one π bonding orbital.

The entries in Table V also allow one to analyze the potential for bonding across the ring. Thus 3A₁' which is so strongly antibonding along the ring framework, shows appreciable (0.023) cross-ring SS bonding. Similarly the bonding orbital 1A'' exhibits significant (0.010) SS interaction. However, this SS bonding character is more than offset by the SS antibonding character of the 1A₂', 2E', 3E', and 2E'' orbitals.

The overlap population for each region is given in the last line of Table V. The overlap population calculated for the nearest neighbors SN is 0.52. This is essentially the same as the value 0.49 we find²⁵ for nearest neighbors in S₄N₄, a system for which a bond order of 1.07 has been calculated.²⁶ Thus, our result for S₃N₃⁻ suggests a net of one bond between nearest neighbors. In view of the preceding discussion it seems reasonable to attribute this to the roughly four to five σ bonds and the approximate one π bond which are distributed over six centers. Further, the cross-ring overlap populations of -0.17 for SS and -0.01 for NN indicate that there is not appreciable transannular bonding. Adkins and Turner¹⁸ have also concluded that there is no appreciable transannular bonding in S₄N₂.

The atomic charges q_r ²⁷ for S₃N₃⁻ were calculated to be $q_S = +0.065$ and $q_N = -0.40$. With the same method we obtained²⁵ $q_S = +0.32$ and $q_N = -0.32$ for S₄N₄, essentially the same value (0.33) which Gopinathan and Whitehead²⁸ found for S₄N₄ using a CNDO procedure. The SCF X_α scattered-wave calculations of Salahub and Messmer²⁹ predict more polar SN bonds ($|q| = 0.56$ in S₄N₄ and $|q| = 0.48$ in S₂N₂) as do the SCF results of Tanaka et al.³⁰ ($|q| = 0.71$ for S₄N₄). Certainly the additional charge in S₃N₃⁻ appears to be distributed mainly on the sulfur centers. However, one must not only bear in mind the method dependence indicated above but also one must remember that there are several different measures of the charge to be associated with an atom.³¹ In any case

the electron-rich centers in S₃N₃⁻ are the nitrogen atoms and, from the partial lone-pair character of the higher MOs (e.g., 2E''), one would predict ready adduct formation with Lewis acids, cf. S₂N₂(BCl₃)_x, $x = 1, 2$,³² and S₄N₄(BF₃)₂,³³ although nucleophilic displacement of halide may well occur in the case of the SN anion.

The UV spectra of all the S₃N₃⁻ salts exhibit a broad, smooth absorption band at 360 nm with ϵ ca. $8 \times 10^3 \text{ M}^{-1} \text{ cm}^{-1}$. A first approximation to the theoretical value corresponding to this transition is given by the difference between unoccupied and occupied one-electron energy levels, $\epsilon_e - \epsilon_i$, which in the HFS method corresponds to the averaged excitation energy $(1/4)(3\Delta E_{\text{triplet}} + \Delta E_{\text{singlet}})$. For the transitions 2E'' \rightarrow 2A₂'' and 2E'' \rightarrow 5E' one obtains values of 399 and 359 nm, respectively. Further insight may be gained by calculating the oscillator strengths. We obtain a ratio of oscillator strengths of ca. 10³ in favor of the 2E'' \rightarrow 2A₂'' transition, thus suggesting that this $\pi^* \rightarrow \pi^*$ transition is responsible for the observed UV absorption band.

Electronic Structure of S₃N₃⁺. The synthesis of S₃N₃Cl, which might be expected to contain the S₃N₃⁺ cation (cf. S₄N₃Cl³⁴ and S₄N₅Cl³⁵), has recently been claimed,³⁶ but attempts to confirm this report in our laboratory have been unsuccessful.³⁷ It was, therefore, of interest to perform calculations for the hypothetical species S₃N₃⁺, in order to assess the likelihood of its existence.

The ab initio HFS-SCF procedure was applied to planar (D_{3h}) S₃N₃⁺. Average S-N distances of 1.55 Å were assumed by comparison with other monocyclic, planar S-N cations, e.g., S₃N₂⁺ (1.58 Å),³⁸ S₄N₃⁺ (1.55 Å),³⁹ and S₅N₅⁺ (1.54-1.56 Å).^{40,41} The orbital energy level ordering for S₃N₃⁺ is the same as for S₃N₃⁻ shown in Figure 2 except for the interchange of the 2A₁' and 1A₂'' levels and the fact that 1E'' level lies below the 3E' level. Each of the degenerate 2E'' HOMOs is singly occupied in S₃N₃⁺, suggesting that this species should be a diradical. This feature of the electronic structure suggests that planar S₃N₃⁺ would be a highly reactive species. Other ring conformations are possible, however, and synthetic routes to S₃N₃⁺, including the controlled oxidation of S₃N₃⁻, are under investigation.

Acknowledgments. The authors are grateful to the National

Research Council of Canada for support in the form of operating grants (T.C. and W.G.L.) and to the Province of Alberta for a scholarship (J.B.). Particular thanks are extended to Dr. Jan Troup, Molecular Structure Corp., Texas, for the X-ray structure determination and to Dr. T. Ziegler for helpful discussions and the use of his computer programs.

Supplementary Material Available: A listing of structure factor amplitudes and a table of intermolecular contacts up to 4 Å (5 pages). Ordering information is given on current masthead page.

References and Notes

- (1) (a) J. Bojes and T. Chivers, *J. Chem. Soc., Chem. Commun.*, 453 (1977); (b) *Inorg. Chem.*, **17**, 318 (1978).
- (2) A. Zalkin, T. E. Hopkins, and D. H. Templeton, *Inorg. Chem.*, **5**, 1767 (1966).
- (3) R. Steudel, F. Rose, R. Reinhardt, and H. Bradaczek, *Z. Naturforsch. B*, **32**, 488 (1977).
- (4) A. J. Banister and H. G. Clarke, *J. Chem. Soc., Dalton Trans.*, 2661 (1972).
- (5) A. J. Banister, *Nature (London) Phys. Sci.*, **237**, 92 (1972).
- (6) D. T. Cromer and J. T. Waber, "International Tables for X-ray Crystallography", Vol. IV, Kynoch Press, Birmingham, England, in preparation.
- (7) D. T. Cromer and D. Liberman, *J. Chem. Phys.*, **53**, 1891 (1970).
- (8) See paragraph at end of paper regarding supplementary material.
- (9) J. C. Slater, *Adv. Quantum Chem.*, **6**, 1 (1972).
- (10) E. J. Baerends, D. E. Ellis, and P. Ros, *Chem. Phys.*, **2**, 41 (1973).
- (11) D. E. Ellis, *Int. J. Quantum Chem.*, **2**, 43 (1968).
- (12) (a) T. Ziegler, A. Rauk, and E. J. Baerends, *Chem. Phys.*, **16**, 209 (1976); (b) *Theor. Chim. Acta*, **43**, 261 (1977); (c) T. Ziegler and A. Rauk, *ibid.*, **46**, 1 (1977); (d) M. Trsic and W. G. Laidlaw, *Can. J. Chem.*, **56**, 1582 (1978); (e) W. G. Laidlaw and M. Trsic, *Chem. Phys.*, in press.
- (13) E. J. Baerends and P. Ros, *Int. J. Quantum Chem.*, in press.
- (14) E. Clementi and C. Roetti, *At. Data Nucl. Data Tables*, **14**, 177 (1974).
- (15) (a) F. P. Boer and W. N. Lipscomb, *J. Chem. Phys.*, **50**, 989 (1969); (b) B. Roos and P. Siegbahn, *Theor. Chim. Acta*, **17**, 199 (1970); (c) F. J. Marsh and M. S. Gordon, *Chem. Phys. Lett.*, **45**, 255 (1977).
- (16) A. J. Banister and J. A. Durrant, *J. Chem. Res. (M)*, 1912 (1978).
- (17) T. Ziegler, private communication.
- (18) R. R. Adkins and A. G. Turner, *J. Am. Chem. Soc.*, **100**, 1383 (1978).
- (19) J. Bojes and T. Chivers, *Inorg. Chem.*, in press.
- (20) J. S. Anderson and J. S. Ogden, *J. Chem. Phys.*, **51**, 4189 (1969).
- (21) R. M. Atkins and P. L. Timms, *Spectrochim. Acta, Part A*, **33**, 853 (1977).
- (22) G. E. Coxon and D. B. Sowerby, *Inorg. Chim. Acta*, **1**, 381 (1967).
- (23) J. Emsley, *J. Chem. Soc. A*, 109 (1970).
- (24) P. O. Offenhartz, "Atomic and Molecular Orbital Theory", McGraw-Hill, New York, 1970. See eq 10.97 for the formula for calculating orbital overlap population, eq 10.98 for overlap population, and eq 10.102 for gross electron charge.
- (25) T. Chivers, L. Fielding, W. G. Laidlaw, and M. Trsic, to be published.
- (26) A. G. Turner and F. S. Mortimer, *Inorg. Chem.*, **5**, 906 (1966).
- (27) The atomic charge is the nuclear charge minus its gross atomic charge; see, for example, ref 24.
- (28) M. S. Gopinathan and M. A. Whitehead, *Can. J. Chem.*, **53**, 1343 (1975).
- (29) D. R. Salahub and R. P. Messmer, *J. Chem. Phys.*, **64**, 2039 (1976).
- (30) K. Tanaka, T. Yamabe, A. Tachiban, H. Kato, and K. Fukui, *J. Phys. Chem.*, **82**, 2121 (1978).
- (31) R. S. Mulliken, *J. Chem. Phys.*, **23**, 1833 (1955).
- (32) R. L. Patton and W. L. Jolly, *Inorg. Chem.*, **8**, 1392 (1969).
- (33) M. Goehring, H. Herb, and H. Missemeyer, *Z. Anorg. Allg. Chem.*, **267**, 238 (1952).
- (34) A. W. Cordes, R. F. Kruh, and E. K. Gordon, *Inorg. Chem.*, **4**, 681 (1965).
- (35) T. Chivers and L. Fielding, *J. Chem. Soc., Chem. Commun.*, 212 (1978).
- (36) L. Zborilova, J. Touzin, D. Navratilova, and J. Mrksova, *Z. Chem.*, **12**, 27 (1972).
- (37) T. Chivers and L. Fielding, unpublished observations.
- (38) R. J. Gillespie, P. R. Ireland, and J. E. Vekris, *Can. J. Chem.*, **53**, 3147 (1975).
- (39) T. N. Guru Row and P. Coppens, *Inorg. Chem.*, **17**, 1670 (1978), and references cited therein.
- (40) H. W. Roesky, W. Grosse-Bowing, I. Rayment, and H. M. M. Shearer, *J. Chem. Soc., Chem. Commun.*, 735 (1975).
- (41) A. J. Banister, J. A. Durrant, I. Rayment, and H. M. M. Shearer, *J. Chem. Soc., Dalton Trans.*, 928 (1976).
- (42) A weak band at ca. 950 cm^{-1} , previously reported for the infrared and Raman spectra of $\text{Cs}^+\text{S}_3\text{N}_3^-$,^{1b} has not been observed in the spectra of samples that have been prepared subsequently.

Photolytic Separation of Carbon Isotopes in Cryogenic Solutions of Carbon Disulfide

Samuel M. Freund, William B. Maier II, Redus F. Holland, and Willard H. Beattie*

Contribution from the University of California, Los Alamos Scientific Laboratory, P.O. Box 1663, Los Alamos, New Mexico 87545. Received October 16, 1978

Abstract: We report the separation of carbon isotopes by photolysis of CS_2 in cryogenic solutions of nitrogen, krypton, and argon with 206-nm light from an iodine resonance lamp. The spectral distribution of the ultraviolet absorption depends on solvent. Thus, in liquid nitrogen the photolytic rate of $^{13}\text{CS}_2$ is greater than that of $^{12}\text{CS}_2$, whereas in liquid krypton and liquid argon the reverse is true.

Introduction

Recent success in the separation of D from H in cryogenic solutions of formaldehyde in our laboratory¹ has stimulated interest in extending the technique to the separation of isotopes of other light elements.² The concurrent vapor-phase isotope separation of carbon isotopes from the low-pressure photolysis of CS_2 with light from an ArF laser,³ the existence of predissociative states which give rise to well-defined vibronic structure in the region 185–215 nm,^{4–8} and the availability of a convenient and powerful resonance lamp photolysis source^{6,9} suggested that CS_2 might be a suitable candidate for a liquid-phase separation.

In this paper we report the photolytic separation of carbon isotopes in cryogenic solutions of CS_2 in nitrogen, krypton, and argon with 206-nm light from an iodine resonance lamp.

The ultraviolet absorption spectrum of carbon disulfide is

different in different solvents, so that the photodestruction rates of $^{12}\text{CS}_2$ relative to $^{13}\text{CS}_2$ can easily be varied.¹⁰

Experimental Section

The apparatus used for both the spectroscopy and the photochemistry experiments have been described in detail in ref 1. Ultraviolet absorption spectra were obtained with a Cary Model 17 spectrophotometer. Photolyses were performed in copper two-way cells. Corning 7940 UV filter material (4 mm thick) was used to pass UV light, and CaF_2 windows allowed simultaneous monitoring of the disappearance of CS_2 with a Perkin-Elmer 180 infrared spectrophotometer. No attempt was made to monitor products.

The $^{12}\text{CS}_2$ concentration was monitored through a 2.6-cm path length at 1531.1 cm^{-1} ($\sigma_{\text{ir}} = 1.63 \times 10^{-16} \text{ cm}^2$) and the $^{13}\text{CS}_2$ at 1481.0 cm^{-1} ($\sigma_{\text{ir}} = 1.31 \times 10^{-16} \text{ cm}^2$). These wavenumbers correspond to the collapsed and shifted ν_3 rotation-vibration band in liquid argon (LAr) at -170°C .¹¹ Here the σ 's are the measured peak ab-